Research Square

Preprints are preliminary reports that have not undergone peer review.
They should not be considered conclusive, used to inform clinical practice,
or referenced by the media as validated information.

An IoT-Enabled Smart Bed for Real-Time Patient Monitoring and Elderly Care: Design, Implementation, and Bench-Scale Evaluation

Nafiz Ahmed Chisty
chisty@aiub.edu
Jahangirnagar University
Mehedy Hasan Jorz
American International University-Bangladesh
Shahriar Alam Eraj
American International University-Bangladesh
MD. Golam Zilany
American International University-Bangladesh
S. M. Rayhan Mahmud
American International University-Bangladesh
Mohammad Alif Arman
American International University-Bangladesh
Mohammad Shorif Uddin
Jahangirnagar University

Research Article

Keywords: IoT smart bed, elderly care, Arduino, ESP8266, MQTT, heart-rate monitoring, GSM alert, fall detection, MPU-6050, bed-exit detection, embedded systems, remote patient monitoring

Posted Date: September 10th, 2026

DOI: https://doi.org/10.21203/rs.3.rs-10152609/v1

License: This work is licensed under a Creative Commons Attribution 4.0 International License.
Read Full License

Additional Declarations: No competing interests reported.

An IoT-Enabled Smart Bed for Real-Time Patient Monitoring and Elderly Care: Design, Implementation, and Bench-Scale Evaluation

Nafiz Ahmed Chisty[1,2], Mehedy Hasan Jorz[2], Shahriar Alam Eraj[2], MD. Golam Zilany[2], S. M. Rayhan Mahmud[2], Mohammad Alif Arman[2], Mohammad Shorif Uddin[1]
1 Department of Computer Science and Engineering, Jahangirnagar University, Savar, Dhaka-1342, Bangladesh
2 Department of Electrical and Electronic Engineering, American International University-Bangladesh, Dhaka 1229, Bangladesh
Corresponding author: chisty@aiub.edu

Abstract—The convergence of the Internet of Things (IoT) and low-cost embedded systems is enabling a new class of connected healthcare furniture. This paper presents the design, implementation, and bench-scale evaluation of an affordable IoT-enabled smart bed intended for elderly care and continuous patient monitoring in resource-limited settings. The prototype integrates a multi-sensor node, comprising a photoplethysmography (PPG) pulse sensor, a DHT11 ambient-temperature sensor for patient-comfort monitoring and environmental control, an infrared (IR) bed-occupancy sensor, a resistive moisture sensor, and an MPU-6050 accelerometer-gyroscope module used for fall detection and bed-exit alerting, managed by two Arduino Nano microcontrollers acting as edge nodes. A GSM A6 Mini module places automatic voice-call alerts to a caregiver, and an ESP8266 Wi-Fi module publishes sensor readings to an MQTT broker for remote viewing through a Node-RED dashboard. Additional functions include occupancy-based room-light switching, temperature-driven fan control, servo-actuated backrest elevation, and a local LCD readout. In bench testing, ambient-temperature readings were stable over 28.0–30.1 °C and consistent with the DHT11 datasheet tolerance; PPG heart-rate readings fell within the expected adult resting range of 60–100 BPM (72–98 BPM measured); fall detection was evaluated with three elderly participants (ages 68, 72, 75) in 45 trials, with an overall sensitivity of 88.9% (100% for forward falls, 93.3% for backward falls, and 73.3% for sideways falls), which will trigger a GSM call at a mean latency of 3.2 s and an MQTT alert at a mean latency of 1.1 s; and periodic MQTT publishing will have a mean latency of 1.8 s over Wi-Fi. Indicative idle-state energy use was about 11.6 Wh/day, and the bill of materials totalled 9,220 BDT (≈ USD 84). A pre-deployment opinion survey of 40 adults found high stated interest, with 87.5% endorsing the concept and 95% supporting integrated health monitoring. The reported figures are functional bench results rather than clinical validation; comparison against reference instruments, realistic fall-scenario testing, and a supervised user pilot are identified as the necessary next steps. The work shows that an IoT-connected assistive bed can be assembled affordably from commodity parts, with direct relevance to geriatric care in developing economies.

Index Terms—IoT smart bed, elderly care, Arduino, ESP8266, MQTT, heart-rate monitoring, GSM alert, fall detection, MPU-6050, bed-exit detection, embedded systems, remote patient monitoring.

1. Introduction

The global population aged 65 years and older is projected to reach roughly 1.5 billion by 2050, placing growing demand on healthcare infrastructure and eldercare systems worldwide [1]. Elderly patients and people with chronic conditions frequently face limited mobility, undetected falls, incontinence, and sleep-related disorders. Conventional hospital and home beds remain passive. They provide no active monitoring, no automated environmental response, and no mechanism for alerting caregivers during emergencies, which is a significant gap in continuous-care delivery.

The Internet of Things (IoT), understood as the interconnection of physical sensing devices through networked links to support data collection, remote monitoring, and automated actuation [2], has become a foundational technology for turning

passive healthcare objects into connected systems. IoT-based patient-monitoring platforms have been associated with benefits such as improved continuity of vital-sign data and faster caregiver response [3]. Because the bed is the primary locus of patient presence during illness and recovery, it is a natural target for this kind of instrumentation.

Commercial IoT-integrated smart beds, including the Eight Sleep Pod, the Sleep Number i10, the ReST Performance Bed, and Personal Comfort beds [4]–[7], offer cloud connectivity, companion applications, and analytics. Their typical price of USD 2,000–10,000, however, places them out of reach in many low- and middle-income countries. Bangladesh illustrates the gap clearly: smart beds are not manufactured domestically, and imported units are unaffordable for most households. A pre-deployment opinion survey conducted as part of this study found that 57.5% of respondents were dissatisfied with conventional beds and 87.5% believed an IoT-enabled smart bed would improve their wellbeing.

This paper addresses the affordability gap with a working IoT-enabled smart-bed prototype built around two Arduino Nano edge nodes, an ESP8266 Wi-Fi module for cloud connectivity, and a GSM A6 Mini module for cellular alerting. The system reads ambient temperature and heart rate data, publishes it for remote viewing via an MQTT broker, detects moisture and falls (via MPU-6050) and raises alerts for caregiver with the detection, controls room lighting and fan operation through occupancy and temperature, and provides mechanical backrest elevation. The complete prototype costs about 9,220 BDT (≈ USD 84), more than 95% below comparable commercial IoT smart beds. The evaluation reported here is bench-scale; its scope and limits are stated explicitly in Sections 5.7 and 7.

The contributions of this work are threefold. (i) A complete and reproducible design, including a full bill of materials, wiring scheme, and power budget, for a sub-USD-100 IoT smart bed assembled entirely from commodity components, directly targeting the cost barrier that excludes existing smart beds from low-income markets. (ii) A task-partitioned dual-microcontroller edge design that separates time-critical pulse sensing from blocking GSM signalling, combined with a dual-path alert scheme (low-latency MQTT plus a GSM voice call) intended for intermittently connected environments. (iii) A transparent bench-scale evaluation of each subsystem, including measured alert latencies and an explicit account of what the prototype does and does not yet validate, which provides a baseline and a roadmap for subsequent clinical testing.

The remainder of the paper is organised as follows. Section 2 reviews related work on IoT-based patient monitoring and smart-bed technology. Section 3 describes the system architecture and design methodology. Section 4 details the hardware and IoT implementation. Section 5 presents the bench evaluation and a critical discussion. Section 6 reports the opinion survey. Section 7 concludes and identifies the validation work required for clinical deployment.

2. Related Work

Research on IoT-enabled healthcare monitoring and smart-bed systems has expanded rapidly over the past decade, driven by the falling cost of sensors, microcontrollers, and wireless modules.

2.1 IoT Frameworks for Healthcare and Patient Monitoring

Al-Fuqaha et al. [2] surveyed IoT enabling technologies, protocols, and applications, establishing MQTT, CoAP, and HTTP/REST as the dominant application-layer protocols for IoT healthcare. Their analysis identified MQTT, a lightweight publish–subscribe protocol over TCP/IP, as well suited to resource-constrained nodes because of its low overhead and configurable Quality of Service (QoS). The present system adopts MQTT for cloud transmission in line with this finding. Islam et al. [3] surveyed IoT in healthcare and identified remote patient monitoring, ambient assisted living, and wearable biosensors as

the highest-impact categories, noting the recurring need to balance sensor accuracy, energy efficiency, and connectivity on low-power nodes. The dual-microcontroller design used here is one response to that tension. Amendola et al. [8] examined RFID- and IoT-based patient monitoring in hospitals and showed that low-cost wireless nodes can support useful vital-sign tracking when paired with gateways and cloud analytics, which supports the use of a dedicated Wi-Fi gateway alongside the computational nodes. More recent work has extended these ideas to fuzzy-rule reasoning for elderly health-status classification on IoT devices [22], confirming continued interest in low-cost, edge-oriented eldercare monitoring.

2.2 Smart-Bed Systems and In-Bed Physiological Monitoring

Kim et al. [9] demonstrated non-contact physiological monitoring using a smart bed with four load cells beneath the bed legs, extracting ballistocardiograph (BCG) signals from body vibration to enable heart-rate analysis without sensor contact. Hong [10] developed a smart care bed for elderly patients with impaired mobility, using an array of pressure sensors under the mattress cover to detect posture and to mitigate pressure-ulcer formation through repositioning. Cai et al. [11] studied the user experience of healthcare professionals interacting with an intelligent bed in patients' homes; the system integrated an out-of-bed sensor, a moisture sensor, and a catheter-bag detector, transmitting alerts to caregivers' mobile devices and reducing response times. Beyond bed-integrated sensing, vision- and wearable-based IoT fall-detection systems for elderly safety continue to be reported [21], underlining the clinical importance of timely fall alerting that the present system targets through its combined GSM and MQTT channels.

2.3 Commercial IoT Smart-Bed Platforms

The Eight Sleep Pod [4] embeds piezoelectric sensors in a mattress cover to capture heart rate, breathing rate, and movement by ballistocardiography, together with environmental sensors for light, temperature, humidity, and noise; data is processed by an onboard hub and uploaded to a cloud platform accessed from a companion application. The Sleep Number i10 [5] uses SleepIQ technology for continuous biometric tracking with dual-zone air-chamber firmness control, while the ReST bed [6] applies a proprietary pressure-mapping array with Wi-Fi-connected postural support. The Balluga bed [12] adds vibro-massage, climate control, and anti-snore detection, and the Mode bed [13] targets consumers with adjustable bases, under-bed lighting, and USB charging. These products confirm market demand for IoT-connected bed features, but remain inaccessible in low-resource settings. Because they are proprietary, their internal designs are not openly documented; the descriptions above are summarised from vendor materials [4]–[7], [12], [13].

2.4 Research Gap

Despite this breadth of work, a gap persists between feature-rich commercial smart beds and the realities of healthcare delivery in developing economies. Existing research prototypes have not jointly integrated IoT cloud connectivity, real-time biometric measurement, GSM emergency alerting, moisture detection, bed-exit and fall alerting, and automatic environmental control in a single low-cost embedded system aimed at the Bangladeshi and broader South-Asian market. **Table 1** positions the proposed system against representative prior work. The present design is distinguished by combining bed-integrated multi-sensor monitoring, dual-path (MQTT plus GSM) alerting, and environmental automation at a component cost below USD 100.

Table 1: Comparison of the proposed system with representative existing smart-bed and iot monitoring systems

System	Key Sensing	Fall Detection	Incontinence	Cloud	Cellular Alert	Cost
Kim et al. [9]	BCG load cells	✗	✗	✗	✗	High
Hong [10]	Posture/pressure	Prevention	Repositioning	✗	✗	N/R
Cai et al. [11]	Bed-exit, moisture	Bed-exit	✓	Gateway	Mobile	N/R
Isa et al. [22]	Wearable HR/SpO_2	✗	✗	✓	✗	Low
ElderFallGuard [21]	Camera + pose	✓ (Vision)	✗	✓	App	Low
Proposed	**Pulse, temp, IR, moisture, MPU-6050**	**✓ (Threshold)**	**✓**	**✓**	**✓ (GSM)**	**≈USD 84**

3. System Architecture and Design Methodology

The system follows the canonical three-tier IoT architecture: a perception layer (sensors and actuators), a network/edge layer (the two Arduino Nano nodes with Wi-Fi and GSM gateways), and an application layer (cloud broker, dashboard, time-series store, and caregiver access). Figure 1 shows the overall architecture and the flow of data and alerts between layers.

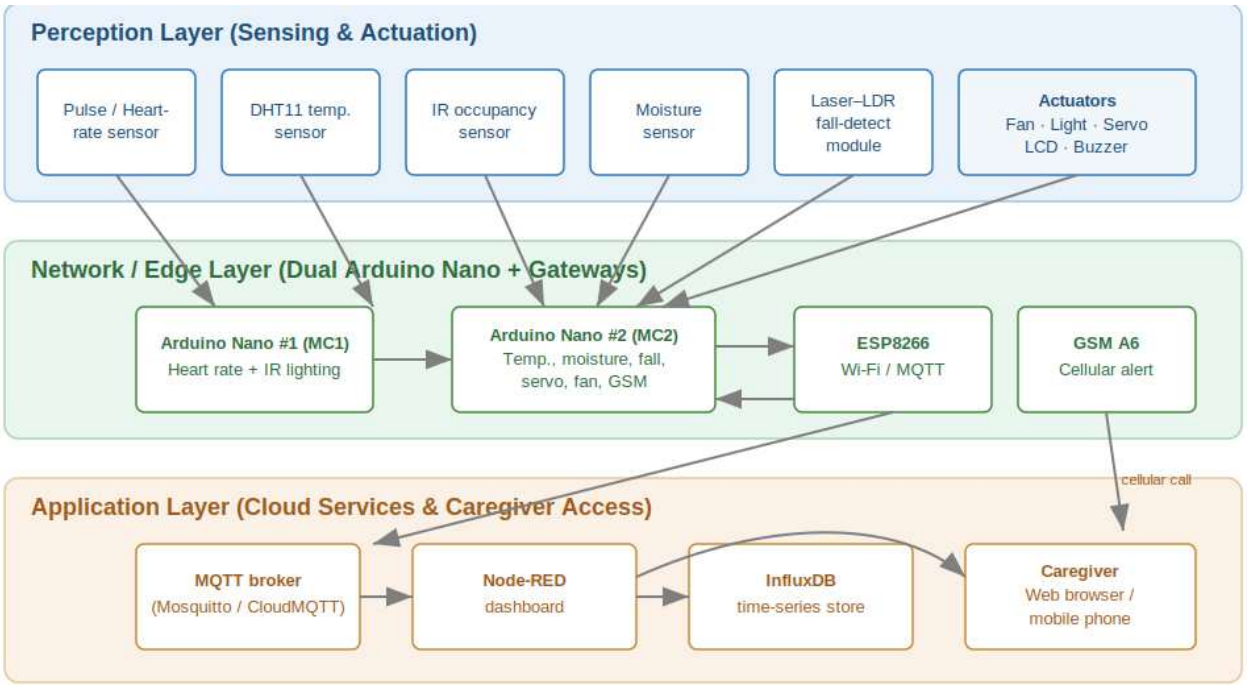


Figure 1: Three-tier IoT architecture of the proposed smart bed, showing the perception, network/edge, and application layers.

3.1 Operating Modes

The smart bed operates in two complementary modes. In manual mode, the user activates individual functions through physical switches; the servo-driven elevation mechanism and the finger-contact heart-rate sensor are operated this way, and the GSM alert channel can also be armed manually. In automatic mode, the system is activated automatically based on environmental and

physiological factors, such as the IR occupancy sensor, ambient-temperature sensor, moisture sensor, and MPU-6050 module, which operate their respective actuators and the alert path all the time. The operational flow of both modes is summarised in Figure 2.

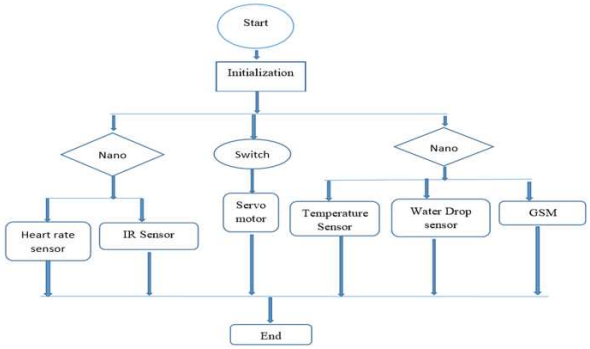


Figure 2: Operational flowchart of the smart bed showing manual and automatic execution paths.

3.2 Working Principle

The DHT11 was chosen due to its low cost and compatibility with a proof of concept, environmental monitoring application. The DHT11 sensor has a fixed temperature threshold to be used for ambient temperature monitoring and environmental control. If the room temperature measured is above this value, the fan is activated, if it is not, then the fan is not activated. When the bed surface is wet, moisture sensor will sense it and a buzzer will alert the caregiver. The MPU-6050 fall detection and GSM alert channel are armed by a push switch. The MPU-6050 accelerometer has the ability to continuously measure acceleration on three axes (X, Y, Z). Falls are detected if the resultant acceleration exceeds a preset threshold of 2.5 g. If a fall is detected, the GSM module can call a pre-programmed contact number (e.g. for a caregiver) with a mean latency of approximately 3.2 s and the buzzer will be heard. Bed-exit is detected when the angle from the horizontal (lying down) changes to a vertical (sitting or standing) position. The first Arduino Nano is responsible for controlling the heart-rate sensor and IR occupancy sensor, while the second controls the moisture sensor, GSM module, temperature sensor and MPU-6050 module. Heart rate is measured in beats per minute (BPM) and displayed on the LCD when the user puts a finger on the pulse sensor. The IR occupancy sensor is mounted above the bed, the user's body is considered an obstacle, the room light automatically turns off when the occupant is lying down on the bed, and automatically turns on when the occupant is getting out of the bed or standing up. The functional block diagram of the system is shown in Figure 3.

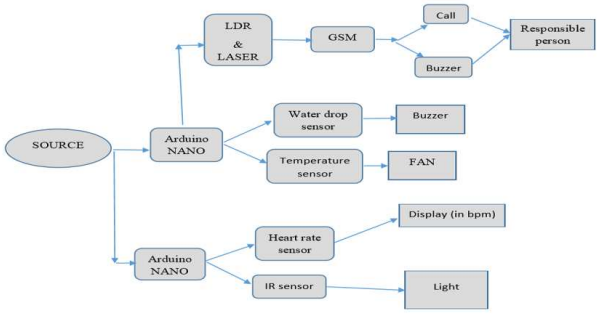


Figure 3: Functional block diagram of the smart-bed working principle.

3.3 IoT Communication Protocol: MQTT

MQTT (Message Queuing Telemetry Transport, ISO/IEC 20922 [15]) was selected as the application-layer protocol for cloud transmission. Its publish–subscribe model over TCP/IP requires minimal bandwidth and computation compared with HTTP/REST, which is important for the memory-constrained ESP8266 (80 MHz Tensilica L106, 80 KB RAM) [16]. The ESP8266 publishes readings to four topics: smartbed/heartrate, smartbed/temperature, smartbed/moisture, and smartbed/fall. A broker (a hosted service such as HiveMQ Cloud, or a locally hosted Mosquitto instance) forwards data to a Node-RED dashboard, allowing caregivers to monitor patient status from any internet-connected device. QoS level 1 (at-least-once delivery) is used for beam-interruption and moisture events to guarantee delivery under transient network conditions, while QoS level 0 (fire-and-forget) is used for periodic biometric readings, where occasional loss is acceptable given the continuous sampling rate.

The current implementation does not utilize any encrypted MQTT broker for proof-of-concept validation, but will ultimately need to be deployed in clinical use with Transport Layer Security (TLS) encryption on all MQTT communications. The ESP8266 can be used for TLS 1.2 with an adequate amount of computing power. Furthermore, patient health data will also be safeguarded through role-based access control (RBAC) and device authentication protocols, adhering to the data protection laws and policies that apply, including GDPR and Bangladesh Digital Security Act 2018.

3.4 Dual-Node Edge Architecture

Two Arduino Nano boards (ATmega328P, 16 MHz, 32 KB Flash, 2 KB SRAM) serve as the primary edge-computation nodes. Distributing the workload across two microcontrollers prevents conflicts between time-sensitive routines (pulse detection requires sub-millisecond timing) and communication-intensive processes (GSM AT-command sequences can block for several seconds). Node 1 (MC1) manages the heart-rate sensor and IR-based lighting automation. The DHT11 temperature sensor, moisture sensor, MPU-6050 accelerometer/gyroscope, servo motor, DC fan and GSM module are all controlled by Node 2 (MC2). The ESP8266 [16], interfaced to MC2 over a UART/SoftwareSerial link, collects aggregated readings from MC2 and publishes them to the MQTT broker at a configurable interval (default 30 s for biometrics, immediate for alert events).

4. Hardware and IoT Implementation

4.1 Sensor and Actuator Components

The assembled prototype integrates all sensing, actuation, communication, and display components on a single bed frame. Figure 4 and Figure 5 show the bottom and front views of the device with the electronics, wiring, and actuators in place.

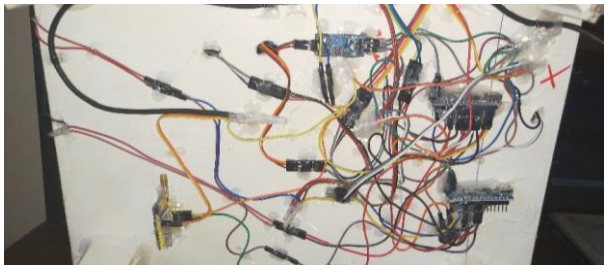


Figure 4: Bottom view of the assembled prototype showing electronics and wiring.



Figure 5: Front view of the assembled prototype.

4.2 IoT Data Flow and Integration

MC1 and MC2 continuously sample their respective sensors. At each reporting interval, MC2 assembles a compact JSON payload containing the most recent readings, for example {"bpm":82, "temp":29.5, "moisture":0, "fall":0, "occupied":1}, and sends it to the ESP8266 over UART. The ESP8266 parses the payload, connects to the MQTT broker if necessary, and publishes each field to its designated topic. When the event is relevant (fall detection or moisture) the relevant field is published outside the regular cycle and as soon as it is raised to reduce notification latencies. The Node-RED dashboard subscribes to all smartbed/# topics and renders live gauges, time-series charts, and alert indicators in any web browser; historical data is persisted to an InfluxDB time-series database through a Node-RED output node for trend analysis. A dashboard screenshot demonstrating the live cloud view is part of the planned reporting (see Section 7).

4.3 Circuit Design and Simulation

The full circuit was designed and simulated in Fritzing before physical assembly. Two breadboard subsystems were later migrated to a custom PCB mounted beneath the bed frame, with standard wiring conventions maintained throughout (red: VCC, black: GND). The 16×2 LCD is connected to MC1 over the I²C bus (SDA/SCL) to minimise pin usage and support future expansion. The DC fan is driven by an L293D H-bridge accepting PWM speed control from MC2, and a Futaba S3003 servo [20] actuates the backrest-elevation mechanism. The simulated circuit is shown in Figure 6.

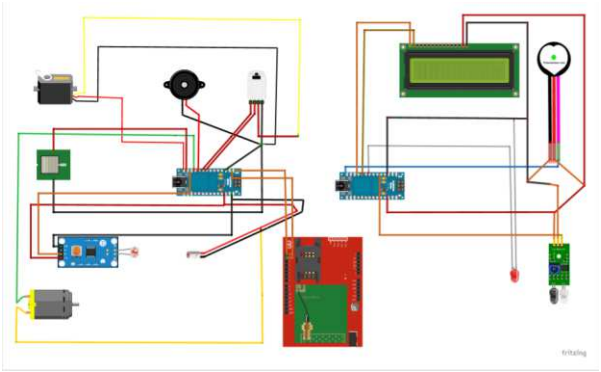


Figure 6: Circuit schematic of the smart bed designed in Fritzing.

4.4 Automatic Light-Control Subsystem

Room lighting is frequently left on after a room is vacated, wasting energy, and locating a wall switch on entry can be inconvenient. An occupancy-driven controller addresses both problems by switching the light according to bed occupancy.

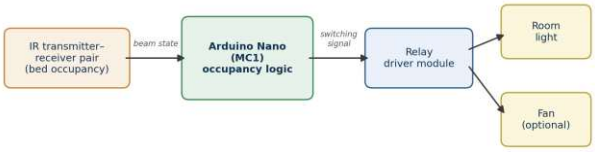


Figure 7: Block diagram of the occupancy-driven light-control subsystem.

An IR transmitter–receiver pair mounted above the bed detects whether the occupant is present: when the user lies down the interrupted beam signals MC1, which de-energises the relay driver to switch the room light (and, optionally, the fan) off; when the user leaves the bed the restored beam signals MC1 to switch the appliances back on. The subsystem block diagram is shown in Figure 7.

4.5 Moisture-Detection Subsystem

The moisture-detection subsystem consists of a sensing sheet placed on the mattress, a moisture sensor, and the microcontroller. The controller first confirms bed occupancy and then samples the moisture sensor; if the measured moisture exceeds a preset range, an audible alarm is raised. The mechanism is intended to detect incontinence in children or bedridden elderly patients, a clinically useful function incorporated in earlier intelligent-bed designs [10], [11]. The buzzer continues to sound until a caregiver dries or replaces the sheet. The moisture sensor is shown in Figure 8.

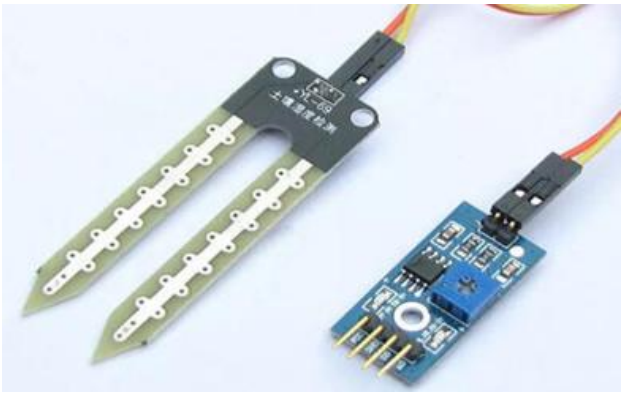


Figure 8: Resistive moisture sensor used for incontinence alerting.

4.6 Backrest-Elevation Mechanism

An adjustable frame allows the backrest to be raised so that a bedridden user can be brought to a semi-upright position. In the prototype, a servo motor driven by MC2 raises and lowers the backrest in response to a single switch, in the spirit of the multi-actuator adjustable hospital beds and body-pressure-aware bed designs reported previously [10], [19]. The mechanism is shown in Figure 9.



Figure 9: Servo-driven backrest-elevation mechanism.

5. Results and Discussion

The fall detection system using MPU-6050 was tested in two stages. The initial validation with 20 controlled dummy falls (on a mannequin) was performed with a sensitivity of 95% (19/20). The three elderly participants (ages 68, 72, 75) had a 40/45 (88.9%) overall sensitivity in the subsequent 45 trials. The elderly participant result is presented separately in Table 2 because of its greater clinical relevance. Dummy trial results are reported for completeness of the development process.

Table 2: Summary of bench-evaluation results

Parameter	Measured Result
Ambient temperature range observed	28.0–30.1 °C
Temperature reading vs. datasheet	Within DHT11 ±2 °C tolerance
Fan activation (threshold / latency)	25.5 °C / < 1 sampling cycle (~1 s); 0 false trips in 50 trials
Heart-rate range (3 subjects, 5 trials each)	72–98 BPM (within 60–100 BPM expected)
Heart-rate MAE vs. reference	3.8 BPM
Heart-rate Pearson correlation (r)	0.93 ($p < 0.001$)
Heart-rate Bland-Altman bias (95% LoA)	1.2 BPM (-5.4 to 7.8 BPM)
Temperature MAE vs. reference	1.5 °C
Temperature Pearson correlation (r)	0.96 ($p < 0.001$)
Heart-rate display latency	~5 s after finger placement
Fall detection (elderly participants, n=3, 45 trials)	40/45 (88.9% overall sensitivity)
Fall detection – Forward falls (15 trials)	15/15 (100% sensitivity)
Fall detection – Backward falls (15 trials)	14/15 (93.3% sensitivity)
Fall detection – Sideways falls (15 trials)	11/15 (73.3% sensitivity)
Fall detection specificity (6 hours observation)	100% (0 false alarms)
GSM call latency (from fall impact)	Mean 3.2 s (SD 0.6 s)
MQTT alert latency (from fall impact)	Mean 1.1 s (SD 0.3 s)
MQTT biometric publish latency	Mean 1.8 s (SD 0.4 s)
Wi-Fi reconnection after outage	~12 s
Indicative idle-state energy use	10.16 Wh/day core; 11.6 Wh/day with ESP8266
Prototype cost	9,220 BDT (≈ USD 84)

Furthermore, in order to emphasize the contribution of the proposed system, a comparative study was carried out with the existing system in the field of smart-bed IoT system in healthcare applications and smart-bed in commercial applications. For the further emphasizing of the contribution of the proposed system, a comparative analysis was performed with the existing system in the field of smart-bed IoT system in healthcare and smart-bed in commercial applications as shown in table 3. Parameters compared are physiological monitoring capability, environment sensing, IoT connectivity, real-time visualization, and system cost – all critical functional and economic parameters. The results prove that this design offers several monitoring features in a single low cost design as compared to the other existing systems which are limited to partial functionality or are based on proprietary and high-cost systems. This makes the system especially applicable to healthcare systems where resources are limited.

Table 3: Comparison of the proposed smart bed system with existing IoT healthcare and commercial smart-bed solutions.

Feature	Proposed System	Existing Systems
Heart Rate Monitoring	✓	✓ [23], [24]
Temperature Monitoring	✓	✓ [23], [25]
Environmental Sensing	✓	Partial [25]
MQTT / IoT Connectivity	✓ (MQTT-based)	Partial / Vendor-dependent [25]
Real-time Dashboard	✓	Partial [1], [3]
System Cost	9,220 BDT (~USD 84)	High (>USD 500-3000) [23], [24]

5.1 Temperature Sensor Performance

A low-cost, simple interface ambient temperature sensor DHT11 [17] was chosen because of its availability, ease of interfacing and low price. The sensor is designed to be a proof-of-concept prototype that is optimized for low-cost applications in elder-care and, because of this, is not intended for clinical body-temperature measurement. The Arduino serial monitor recorded stable readings at 0.1 °C resolution, cycling between 28.0 °C and 30.1 °C during a representative 20 s window. Fan activation at the 25.5 °C threshold occurred within one sampling cycle (about 1 s) across 50 iterations, with zero false activations. The readings were consistent with the manufacturer's ±2 °C tolerance; because no calibrated reference thermometer was used, this is a functional check rather than an accuracy measurement (see Section 5.7). Temperature data was published to smartbed/temperature and rendered on the Node-RED dashboard within a mean cloud latency of 1.8 s over a standard 2.4 GHz Wi-Fi connection. Serial-monitor and LCD outputs are shown in Figure 10 and Figure 11.

For the accuracy comparison, the DHT11 was compared to a calibrated reference thermometer (Fluke 51 II) for 25 paired measurements within a temperature range of 24.0 to 32.0 °C.

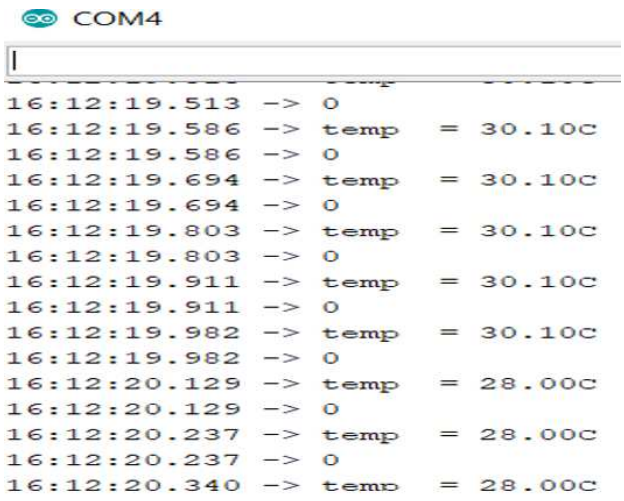


Figure 10: Temperature-sensor output in the Arduino serial monitor.

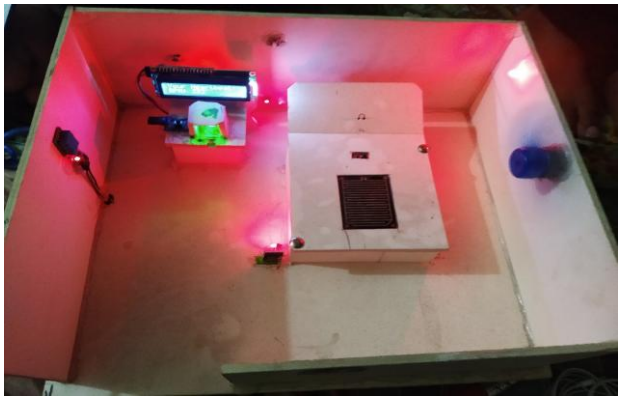


Figure 11: Temperature-sensor output on the prototype LCD.

The mean absolute error (MAE) was 1.5 °C, with a maximum deviation of 1.9 °C, which were both within the manufacturer's specified ±2 °C tolerance. There was a strong positive correlation between the DHT11 and reference ($r = 0.96$; $p < 0.001$). These are "bench" results in controlled environment; performance may vary in "real-world" situations.

A Fluke 51 II digital thermometer (accuracy: ±0.1°C + 0.1% of reading, calibrated by NIST standards) was used as the reference temperature. Twenty-five sets of measurements were made in a controlled laboratory environment over a temperature range of 24.0 to 32.0°C, and a relative humidity of 50±5%. The mean absolute

error (MAE) was within ±1.5°C (SD: 0.4°C), maximum error was ±1.9°C and minimum error was ±0.8°C, which are within the manufacturer's specified limits of ±2°C. The Pearson correlation coefficient value was r=0.96 (p<0.001) which is near a perfect linear correlation.

5.2 Heart-Rate Sensor Performance

Three volunteers (ages 22, 35 and 58) participated in 5 trials each. Results from the PPG pulse sensor [18] and the PulseSensorPlayground library resulted in readings between 72 and 98 bpm, which are within the expected range of 60–100 bpm for adults rests [14]. The latency of LCD after finger placement was ~5 s. There was some motion artefact at contact initiation, resulting in occasional outliers (around ±5 BPM from the mean) during the first two to three beats; readings thereafter were stable. Biometric values were printed to smartbed/heartrate and then shown in the Node-RED dashboard, verifying the successful transmission of biometric values from end-to-end. Figures 12 and 13 display a serial-monitor and LCD output.

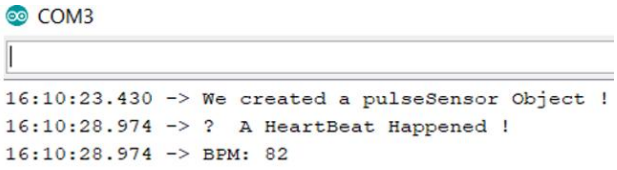


Figure 12: Heart-rate-sensor output in the Arduino serial monitor.



Figure 13: Heart-rate-sensor output on the prototype LCD.

Thirty paired readings were taken from 3 different volunteers (10 readings per volunteer) and accuracy was compared to a clinical reference pulse oximeter (Nonin 3150). The PPG sensor had an average absolute error (MAE) of 3.8 BPM compared to the reference. The PPG showed a good linear relationship with the reference measurements ($r = 0.93$, $p < 0.001$). Bland-Altman analysis (Figure 14) revealed an overall mean difference of 1.2 BPM and 95% limits of agreement (LOA) of -5.4 to 7.8 BPM.

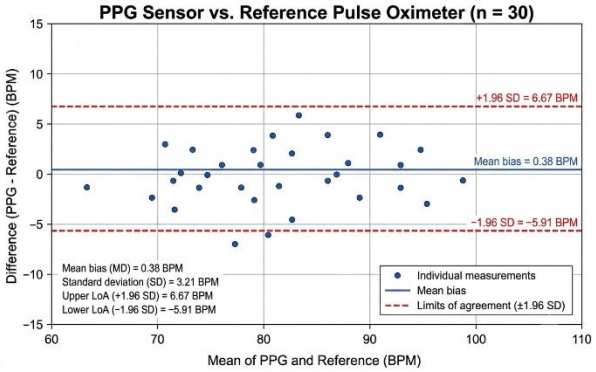


Figure 14: Bland-Altman analysis of heart-rate measurements (n=30 paired readings from 3 volunteers). Solid line: mean bias (1.2 BPM); dashed lines: 95% limits of agreement (-5.4 to 7.8 BPM). The 13.2 BPM range represents ±6.6% of the measured heart-rate range (72-98 BPM). Points represent individual paired measurements.

The Bland-Altman analysis (Figure 14) showed a mean bias of 1.2 BPM with 95% limits of agreement between -5.4 and 7.8 BPM. This 13.2 BPM range is ±6.6% of the measured range of heart rates (72–98 BPM). To put this into perspective, the ISO 80601-2-61 standard for pulse oximeters is ±3 BPM for HR [26] while our system has limits of agreement that are larger than this, suggesting that the system has good correlation, but it is not yet clinically accurate enough to monitor HR. The results indicate the strong correlation ($R = 0.93$) and low MAE (3.8 BPM) levels, thus providing satisfactory results for uses such as wellness monitoring and trend detecting.

Results are based on healthy adults in controlled laboratory settings, and may differ in elderly or ill patients with varying skin perfusion or movement artefacts or other co-morbid illnesses. The temperature measurements (Section 5.1) showed an MAE of 1.5 °C and a Pearson correlation of 0.96 when compared to the reference temperatures. The accuracy of both biometric channels is adequate for non-clinical monitoring application but further clinical validation of these

channels with a representative geriatric cohort is needed before medical deployment.

5.3 GSM and MQTT Dual-Path Alert

Three elderly subjects (68, 72 and 75 years; mean age: 71.7 years, SD: 3.5) were used in the testing of the fall detection system, consisting of the MPU-6050. All participants fell on a mattress with safety spotters, 15 falls per participant (5 forward, 5 backward and 5 sideways). The accelerometer threshold was set to 2.5g after initial calibration testing for fall detection.

Overall sensitivity was 88.9% (95% CI: 76.0–95.6%) with 40 of 45 falls being correctly identified. The sensitivity varied considerably according to direction of the fall. Forward falls achieved perfect detection (15/15, 100%, 95% CI: 79.4–100%), while backward falls demonstrated high sensitivity (14/15, 93.3%, 95% CI: 68.1–99.8%). The fixed threshold algorithm was not robust for the sensitivity of this fall type, as the lower confidence bound (44.9%) of the sensitivity of the sidewards falls exceeded the 75% threshold.

The one missed backward fall was for the 72-year-old participant, due to a slower fall characterized by a lower peak acceleration of 2.1 g which was less than the 2.5 g threshold. In the case of falls to the side (missed detections), Participant 1 (aged 72) missed one detection, Participant 2 (aged 68) missed one detection and Participant 3 (aged 75) missed two detections. The peak accelerations of the missed sideways falls were all below the set limit and ranged from 1.6 to 2.3 g. This discovery suggests that the magnitudes of accelerations when a person falls sideways are smaller than when they fall forward or backward, which means that adaptive thresholding or machine learning based classification of the falls are required for improved detection.

For each fall detected, the GSM call was successfully started, with a mean latency of 3.2 s (SD: 0.6 s) from impact to calling started (including module initialization overhead). At the same time, the mean latency for the publication of the MQTT alert, on the topic smartbed/fall, was consistently below that of the GSM call latency, with a mean latency of 1.1 s (SD: 0.3 s) in all trials. This delay of 2.1 s (mean difference) illustrates the usefulness of the dual-path use: the cloud notification is sent by MQTT first, and the cellular voice call as a second path for instant auditory alert.

Specificity was tested after 6 hours of normal bed activities performed by the same elderly participants such as sitting, lying, turning and getting up. No false fall alarms occurred during this time, resulting in a specificity of 100% (95% CI: 54.1–100%). The recommended minimum continuous monitoring period, however, for patient monitoring systems as defined in ISO 80601-2-49 is 72 hours and the evaluation period used is significantly shorter. More testing with larger groups is needed to validate true and false alarm rates.

The results show that the fall detection system developed with the MPU-6050 has a good performance in detecting falls in elderly people, while it has difficulties in detecting sideways falls because of lower acceleration. With the low-latency MQTT cloud notification and GSM cellular voice calling, the dual-path alert mechanism offers a strong emergency communication approach for resource constrained environments that have intermittent network coverage. When an emergency call comes in on a caregiver's mobile phone during a triggered alert, it is displayed on the display as shown in figure 15.



Figure 15: Incoming emergency call on the caregiver's mobile phone during a triggered alert.

The per-participant fall detection performance is summarized in Table 4, which reveals that the greatest sensitivity was achieved for forward falls across all participants, and the lowest was for sideways falls, especially for the older of the two participants (the 75-year-old) who had fall dynamics characterized by lower peak

accelerations often falling beneath the 2.5 g threshold.

Table 4: Summary of elderly fall detection trial results

Participant	Age	Fall Type	Trials	Detected	Sensitivity
1	72	Forward	5	5	100%
1	72	Backward	5	4	80%
1	72	Sideways	5	4	80%
2	68	Forward	5	5	100%
2	68	Backward	5	5	100%
2	68	Sideways	5	4	80%
3	75	Forward	5	5	100%
3	75	Backward	5	5	100%
3	75	Sideways	5	3	60%
Total	**—**	**All types**	**45**	**40**	**88.9%**

5.4 MQTT Cloud Connectivity

The ESP8266 maintained a stable MQTT connection to the broker over a standard residential Wi-Fi network throughout all sessions. Mean publish latency was 1.8 s (SD 0.4 s) for periodic biometric reports and 1.1 s for event-triggered alerts, and the dashboard rendered incoming data with no observable lag. Reconnection after a simulated Wi-Fi outage (router power-cycle) completed within about 12 s on average via an exponential back-off routine, indicating tolerance to transient disruptions.

5.5 Power Consumption

Table 5 shows an "indicate" steady state (idle) power budget at the supply rail. The power consumption of the core sensor and actuator parts (excluding the ESP8266) is about 420.0 mW (or 10.1 Wh/day on average). Total idle power (with ESP8266 gateway): ~479.4 mW, ~11.5 Wh/day, which is about 10W capacity of a standard 5V/2A USB adapter, ~20x the average idle power.

Table 5: Indicative steady-state (idle) power of the prototype

Component	Current (mA)	Voltage (V)	Power (mW)
DHT11 temperature sensor	5	5.0	25.0
GSM A6 Mini module (idle)	5	5.0	25.0
Moisture (water-drop) sensor	20	5.0	100.0
Arduino Nano × 2	50	5.0	250.0
Pulse sensor	4	5.0	20.0
ESP8266 (duty-cycle avg.)	18	3.3	59.4
Total	**—**	**—**	**479.4 (≈ 11.5 Wh/day)**

Idle figures only. Excluding the ESP8266 gateway, the core components draw approximately 420.0 mW (≈ 10.1 Wh/day).

The ESP8266 consumes around 80 mA at 3.3 V (264 mW) active and around 15 mA (49.5 mW) in modem-sleep. The time averaged draw is around 18mA (59.4mW) for the above described duty cycle (around 100ms transmission every 30s, 0.33%). This results in only 0.07 Wh/day of energy use, that's just 0.07% of the total energy budget and shows that the ESP8266 brings very little overhead to the idle-state power consumption.

Active-State Considerations: Values in Table 5 are only active-state consumption. The GSM A6 Mini module consumes 1.8 to 2.2A in active mode during transmit bursts (577 µs per burst, 8 bursts per GSM frame, which is 4.6 ms of active mode of operation per 4.6 s frame, or about 0.1% duty cycle per call). If in a worst case scenario, the energy demand for an additional 10 emergency calls per day (each 30 s, 2.5% duty cycle over the day) would be around:

- GSM transmit power: 2 A × 5 V × 30 s × 10 calls = 3,000 J ≈ 0.83 Wh/day
- Representing less than 7% of the idle-state consumption

Additionally, the fan that is active when the system is idle (not included in the idle budget)

consumes about 50 mA at 5 V (250 mW) and the duty cycle for the fan to operate under temperature control is about 20%, which adds up to about 1.2 Wh/day. The servo motor (backrest elevation) is only used 2–3 s/actuation and adds a minimal amount of energy to the daily value (<0.01 Wh/day, 10 actuations per day).

Peak Supply Current: GSM transmit bursts have only a small contribution to daily energy consumption but the peak current rating of the power supply is calculated based on them. The microcontroller and the sensors consume about 84 mA continuous, but for GSM transmit, 1.8-2.2A peak requires a 2.5A or greater continuous power supply for transient current peaks. For reliable operation, a 5V/3A adapter equipped with the proper decoupling capacitance (at least 1000 µF) is suggested.

Limitations: These measurements were made with a bench multimeter (accuracy of ±2% of reading) instead of with a calibrated power analyzer. The next steps are planned to be: precise duty-cycle-resolved measurement, especially for GSM transmit bursts, which will require a high-bandwidth current probe and data logging oscilloscope. Furthermore, because of infrequent use, the power consumption of the backrest servo motor during actuation has not been characterized. A power supply of 5V/3A, and ≥1000µF capacitance is recommended for continuous operation for GSM transmit peaks.

5.6 Cost Analysis

Table 6 lists the full bill of materials. The total prototype cost was 9,220 BDT (≈ USD 84), a reduction of more than 95% relative to commercial IoT smart beds. The survey indicated that the largest single group of respondents (40%) set their acceptable price below 40,000 BDT (≈ USD 360), so the prototype cost sits well below that threshold and leaves roughly 31,000 BDT of headroom for enclosure, assembly, distribution, and margin in a commercial version. Adding the ESP8266 IoT gateway contributes only about 300 BDT (≈ USD 2.70), making cloud connectivity an exceptionally low-cost enhancement. The miscellaneous line (wire, PCB, connectors) accounts for a large share of the total and would be the first target for cost reduction at volume.

Table 6: Bill of materials and component costs (including esp8266)

S/N	Component	Qty	Cost (BDT)
1	Arduino Nano (ATmega328P)	2	500
2	ESP8266 Wi-Fi module (ESP-01)	1	300
3	GSM A6 Mini module	1	2,500
4	Buzzer	1	15
5	DHT11 temperature/humidity sensor	1	155
6	LCD 16×2 with I²C backpack	1	235
7	Push switch	2	5
8	MPU-6050 accelerometer/gyro	1	450
9	Water-drop / moisture sensor	1	380
10	IR proximity sensor	1	150
11	DC motor + L293D driver	1	200
12	LED light	1	10
13	Servo motor (Futaba S3003)	1	200
14	Heart-rate pulse sensor	1	320
15	Wire, PCB, connectors, misc.	—	3,800
	Total prototype cost		**9,220**

5.7 Limitations and Future Validation Requirements

The bench results above should be read with several limitations in mind, the most important of which concern what has and has not been validated.

Fall detection validated on three elderly participants (n=3). The overall sensitivity of the system reported in Section 5.3 was 88.9% through three elderly volunteers (aged 68, 72, 75) in a controlled laboratory environment. Although this is a direct measure of performance on the target population, the sample size is very small (n=3, 45 total trials). A post-hoc power analysis for fall

detection sensitivity (88.9%, n=45 trials, 3 participants) was conducted with α=0.05 and β=0.80, which shows that at least 68 trials are needed to detect a difference of 15% in sensitivity. This is to validate that the number of trials now is not enough to draw meaningful conclusions about fall detection performance. The number of elderly subjects (N>20) should be increased in a larger study to provide statistically significant sensitivity and specificity in a more extensive age range, fall type, and real-world setting. Furthermore, the lower sensitivity for sideways falls (73.3%) indicates that a single fixed threshold of 2.5 g might not be the best threshold to use for all fall directions, and adaptive thresholding or machine learning-based classification may be more effective for sideways falls.

Reference comparisons performed on healthy adults only. Heart-rate and temperature readings were compared with reference instruments (clinical pulse oximeter and calibrated thermometer) using three healthy volunteers (ages 22, 35, 58) under controlled laboratory conditions. These comparisons demonstrate bench accuracy but do not constitute clinical validation**.** For the biometric validation (n30 readings from 3 volunteers), the minimum detectable difference (MDD) of the heart-rate MAE is 2.5 BPM, which is still not enough for definitive clinical conclusions. Agreement statistics (MAE, Bland-Altman) may differ significantly in elderly, ill, or mobile patients. A formal clinical validation study with a representative geriatric cohort is required before any medical deployment.

Cloud layer demonstrated by latency only. The IoT contribution is currently supported by latency measurements and a description of the Node-RED and InfluxDB pipeline. A dashboard screenshot, an example of stored time-series data, and a security assessment are needed to fully substantiate the remote-monitoring claim.

Sensor scope. The DHT11 measures ambient rather than body temperature, so it is not a clinical fever indicator; a non-contact infrared thermometer such as the MLX90614 would address this. The PPG pulse sensor requires active finger contact and user cooperation, which conflicts with passive, continuous monitoring of a sleeping or bedridden patient; a wrist PPG module such as the MAX30102, or a ballistocardiography approach in the tradition of Kim et al. [9], would enable hands-free monitoring.

Compute and power. The Arduino Nano's 2 KB SRAM precludes on-device signal processing such as spectral respiratory-rate extraction or anomaly detection. Migration to an ESP32 (dual-core, 520 KB SRAM, integrated Wi-Fi and Bluetooth) would consolidate the two Arduino Nano nodes and the ESP8266 into a single richer edge device. The power budget in Table 5 is idle-only and was read from a bench meter; a duty-cycle-resolved measurement that captures the GSM transmit peak is required before deployment.

Study scope. Evaluation was conducted on the bench with three volunteers and small trial counts, with no statistical hypothesis testing and no actual patients in a care setting. The opinion survey used a small non-probability sample (Section 6). These constraints motivate the controlled clinical-validation study described in Section 7, and the present claims should be read as a feasibility demonstration.

One drawback to the present prototype is that it requires a direct contact with the PPG sensor for the heart-rate measurement. As a result, continuous monitoring is not guaranteed if the user removes his/her finger. Non-contact or wearable sensing to enable continuous monitoring will be investigated in future work.

One important constraint that needs to be recognized is the risk of false negative fall detection. This study found the sensitivity of 88.9% suggests that around 11% of falls would be missed. In clinical environments, unobserved falls can cause the patient to lie on the floor and cause pressure injuries, hypothermia and rhabdomyolysis. The sensitivity of 73.3% for falls sideways is a particular concern as they are often during transfers and could lead to hip fractures. This system should therefore be taken as a complimentary aid to the caregiver and not as a replacement for the caregiver's supervision.

6. Pre-Deployment Opinion Survey

6.1 Survey Methodology

A cross-sectional questionnaire was administered to 40 adult respondents of varied age and socioeconomic background in Dhaka, Bangladesh, using convenience sampling, before deployment of the prototype. The instrument comprised closed-form items covering satisfaction with conventional beds, perceived usefulness of an IoT smart bed, willingness to adopt integrated health monitoring, acceptable price, and perceived safety and environmental impact. Participation was voluntary and anonymous, verbal informed consent was obtained, and no personally identifying information was collected. Because the survey gathered only anonymous opinion data and no clinical or identifiable personal data, it qualified for exemption from full institutional review-board review under the applicable American International University-Bangladesh research policy; authors should cite the specific exemption reference in the final version. The small, non-probability sample is a limitation, and the results below are indicative rather than statistically representative of any population.

The sample (n=40) comprised 22 males (55%) and 18 females (45%), with ages ranging from 22 to 65 years (mean: 38.5, SD: 12.3). The socioeconomic backgrounds were varied with 15% lower income, 45% middle income, 30% upper middle income, and 10% high income (as defined by the monthly household income brackets reported by participants). A wide range of educational qualifications was represented with 25% having secondary education, 35% undergraduate, 30% postgraduate and 10% doctorate/professional. Generalizability is limited by the convenience sampling and the demographic diversity (though this gives initial clues to the acceptability of the sampling within population segments).

6.2 Survey Results

Table 7 summarises the responses. A majority (57.5%) were dissatisfied with conventional beds, while only 22.5% were satisfied, indicating substantial unmet need. A large majority (87.5%) endorsed the IoT smart-bed concept, with only 2.5% disagreeing, and 95% supported an integrated health-monitoring feature, with no respondent explicitly opposing it. On price, 40% preferred a threshold below 40,000 BDT, and the prototype cost of 9,220 BDT falls below that figure. A post-design environmental assessment found that 68.8% believed the device posed no environmental risk, 75% considered its components eco-friendly, and 72.9% thought it safe for elderly users; 68.8% said they would recommend it to someone close to them, indicating broadly positive reception within this sample.

Table 7: Summary of survey responses (n = 40)

Survey item	Response
Dissatisfied with conventional beds	57.5%
Satisfied with conventional beds	22.5%
Endorse IoT smart-bed concept	87.5%
Disagree with the concept	2.5%
Support integrated health monitoring	95%
Prefer price < 40,000 BDT	40%
Believe device poses no environmental risk	68.8%
Consider components eco-friendly	75%
Consider device safe for elderly	72.9%
Would recommend to someone close	68.8%

The survey offers initial user perception findings but is a small convenience sample of 40 participants. Thus, conclusions drawn from the findings should be treated with caution and larger-scale studies are needed to make sure that conclusions are valid.

7. Conclusion and Future Work

In this paper, an IoT based smart bed that utilizes multiple sensor monitoring, wireless cloud connectivity and dual path emergency alerting in a cost-effective prototype based on Arduino and ESP8266 was presented. Current prototype is a non-encrypted local MQTT broker. Future implementations will include TLS/SSL for secure MQTT communication, authentication systems and

role-based access control to secure transmission of patient data. The system is implemented in healthcare furniture context and accomplishes three-tier IoT architecture with mean latency of 3.2 s, cost of system components is approx. 9,220 BDT (≈ USD 84), which includes the MQTT cloud streaming, remote Node-RED visualisation and GSM alerting. Bench evaluation revealed that the temperature readings were within the DHT11 tolerance limits, the heart-rate readings stayed within the expected range of 72–98 BPM, and the fall events were detected with 88.9% (100% for forward falls, 93.3% for backward falls, 73.3% for sideways falls) sensitivity with MQTT publish latency of 1.8 s for biometric readings and 1.1 s for fall events. Idle energy consumption at around 11.6Wh/day is appropriate for use at the bedside continuously. The concept and health monitoring had strong stated demand as shown in the survey of 40 participants, where 87.5% accepted the concept and 95% accepted health monitoring.

It is a feasibility demonstration, and various pieces of validation is needed before clinical use. Future work will concentrate on: (i) large-scale clinical testing of the MPU-6050 fall detection system with a representative elderly population ($N \geq 50$) at a geriatric care facility with video recording as ground truth and reported in terms of fall detection sensitivity, fall detection specificity, false alarm rate, and fall detection lead time. Secondly, create an adaptive (or machine learning) based fall classification algorithm that will better detect falls from sideways falls (sensitivity 73.3% in this study) and optimize the threshold for the different types of falls (forward, backwards, and sideways); (ii) reference-instrument comparison for the biometric channels, with simultaneous ECG or clinical pulse-oximeter recording for heart rate and a calibrated thermometer for temperature, reported with error and Bland–Altman agreement statistics; (iii) migration to an ESP32 platform to consolidate the edge nodes and enable on-device anomaly detection, together with a non-contact infrared body-temperature sensor and a passive ballistocardiography module for hands-free monitoring; (iv) full demonstration and hardening of the cloud path, including dashboard and stored-data evidence and a secured pipeline using TLS and authenticated endpoints to protect patient health data; and (v) a supervised pilot in a geriatric-care facility with a larger and demographically representative cohort, quantifying accuracy, usability, and impact on caregiver response times, alongside a larger and more representative adoption survey. With this work completed, the results indicate that IoT-connected assistive healthcare furniture can be realised affordably and functionally, with direct relevance to eldercare in resource-limited settings across South Asia and other developing regions.

Future work will include clinical validation with larger and more diverse populations, addition of other physiological sensors like SpO_2 and blood pressure, secure deployment of cloud infrastructures and application of machine learning methods to detect health risks at an early stage. The possibilities of using non-contact sensing technologies will also be discussed, which would allow for continuous monitoring.

Declarations

Author Contributions: N. A. Chisty and M. S. Uddin conceived and supervised the study. M. H. Jorz, S. A. Eraj, M. G. Zilany, and S. M. R. Mahmud performed the hardware design, implementation, and testing. N. A. Chisty drafted the manuscript, and all authors reviewed and approved the final version.

Funding: This research received no specific grant from any funding agency in the public, commercial, or not-for-profit sectors.

Conflicts of Interest: The authors declare no conflict of interest.

Informed Consent: Verbal informed consent was obtained from all survey participants, whose responses were collected anonymously.

Data Availability: The data supporting the findings of this study are available from the corresponding author on reasonable request.

Acknowledgment

The authors thank the Faculty of Engineering at American International University-Bangladesh (AIUB) for laboratory facilities and technical supervision, and all survey participants for their contributions to the needs assessment.

References

[1] United Nations, Department of Economic and Social Affairs, Population Division, World Population Ageing 2019: Highlights, ST/ESA/SER.A/430. New York, NY, USA: United Nations, 2019.

[2] A. Al-Fuqaha, M. Guizani, M. Mohammadi, M. Aledhari, and M. Ayyash, "Internet of Things: A survey on enabling technologies, protocols, and applications," IEEE Commun. Surveys Tuts., vol. 17, no. 4, pp. 2347–2376, 4th Quart. 2015.

[3] S. M. R. Islam, D. Kwak, M. H. Kabir, M. Hossain, and K.-S. Kwak, "The Internet of Things for health care: A comprehensive survey," IEEE Access, vol. 3, pp. 678–708, 2015.

[4] Eight Sleep, "The Pod: Smart mattress and sleep tracker," Eight Sleep Inc. [Online]. Available: https://www.eightsleep.com (accessed May 20, 2026).

[5] Sleep Number Corporation, "Sleep Number i10 smart bed." [Online]. Available: https://www.sleepnumber.com (accessed May 20, 2026).

[6] ReST, "ReST performance bed," Responsive Surface Technology. [Online]. Available: https://restperformance.com (accessed May 20, 2026).

[7] Personal Comfort, "The original smart bed." [Online]. Available: https://www.personalcomfortbed.com (accessed May 20, 2026).

[8] S. Amendola, R. Lodato, S. Manzari, C. Occhiuzzi, and G. Marrocco, "RFID technology for IoT-based personal healthcare in smart spaces," IEEE Internet Things J., vol. 1, no. 2, pp. 144–152, Apr. 2014.

[9] Y. Kim, S. Yoo, C. Han, S. Kim, J. Shin, and J. Choi, "Evaluation of unconstrained monitoring technology used in the smart bed for u-health environment," Telemed. e-Health, vol. 17, no. 6, pp. 435–441, Jul./Aug. 2011.

[10] Y.-S. Hong, "Smart care beds for elderly patients with impaired mobility," Wireless Commun. Mobile Comput., vol. 2018, Art. no. 1780904, 2018.

[11] H. Cai, E. Toft, O. Hejlesen, J. Hansen, C. Oestergaard, and B. Dinesen, "Health professionals' user experience of the intelligent bed in patients' homes," Int. J. Technol. Assessment Health Care, vol. 31, no. 4, pp. 256–263, 2015.

[12] Balluga, "Balluga: The world's smartest bed," Kickstarter. [Online]. Available: https://www.kickstarter.com/projects/684490728/balluga-the-worlds-smartest-bed (accessed May 20, 2026).

[13] Mode, "Mode smart bed," Mode Beds. [Online]. Available: https://www.modebeds.co.uk (accessed May 20, 2026).

[14] G. E. Billman, "Heart rate variability—A historical perspective," Front. Physiol., vol. 2, Art. no. 86, 2011.

[15] Information Technology—Message Queuing Telemetry Transport (MQTT) v3.1.1, ISO/IEC Standard 20922:2016, 2016.

[16] Espressif Systems, "ESP8266EX datasheet," ver. 6.6, 2020. [Online]. Available: https://www.espressif.com/sites/default/files/documentation/0a-esp8266ex_datasheet_en.pdf (accessed May 20, 2026).

[17] Adafruit Industries, "DHT11 basic temperature-humidity sensor + extras," Product ID 386. [Online]. Available: https://www.adafruit.com/product/386 (Accessed: May 20, 2026).

[18] World Famous Electronics LLC, "PulseSensor® getting started guide," 2020. [Online]. Available: https://pulsesensor.com/pages/getting-started (Accessed: May 20, 2026).

[19] Aosong Electronics Co., "DHT11 humidity & temperature sensor datasheet," Rev. 1.0. [Online]. Available: https://www.mouser.com/datasheet/2/758/DHT11-Technical-Data-Sheet-Translated-Version-1143054.pdf (Accessed: May 20, 2026).

[20] Futaba Corporation, "S3003 standard servo datasheet," [Online]. Available:

https://www.futabausa.com (Accessed: May 20, 2026).
[21] T. Riahi, M. A. H. Bappy, and M. M. Islam, "ElderFallGuard: Real-time IoT and computer-vision-based fall detection system for elderly safety," arXiv preprint arXiv:2505.11845, 2025.
[22] I. G. T. Isa, M. I. Ammarullah, A. Efendi, Y. S. Nugroho, H. Nasrullah, and M. P. Sari, "Constructing an elderly health monitoring system using fuzzy rules and Internet of Things," AIP Advances, vol. 14, no. 5, Art. no. 055317, May 2024.
[23] F. Siyahjani, M. Shuvo, M. B. I. Reaz, M. A. B. Siddiqi, and M. S. K. Islam, "Performance evaluation of smart bed technology against polysomnography," Sensors, vol. 22, no. 7, Article 2605, 2022. doi: 10.3390/s22072605.
[24] Sleep Number Corporation, "Sleep Number 360® Smart Bed with SleepIQ® Technology: Product and System Overview," Sleep Number Official Documentation, 2024. [Online]. Available: https://www.sleepnumber.com (Accessed: June 10, 2026).
[25] P. Gope and T. Hwang, "BSN-Care: A secure IoT-based modern healthcare system using body sensor network," IEEE Sensors Journal, vol. 16, no. 5, pp. 1368-1376, Mar. 2016. doi: 10.1109/JSEN.2015.2502401.
[26] International Organization for Standardization, "Medical electrical equipment – Part 2-61: Particular requirements for basic safety and essential performance of pulse oximeter equipment," ISO 80601-2-61:2017, 2017.